Fibroblast growth factor receptor 1 oncogene partner as a novel prognostic biomarker and therapeutic target for lung cancer

Yuria Mano,[1] Koji Takahashi,[1] Nobuhisa Ishikawa,[1] Atsushi Takano,[1] Wataru Yasui,[2] Kouki Inai,[3] Hitoshi Nishimura,[4] Eiju Tsuchiya,[5] Yusuke Nakamura[1,6] and Yataro Daigo[1]

[1]Laboratory of Molecular Medicine, Human Genome Center, Institute of Medical Science, The University of Tokyo, 4-6-1 Shirokanedai, Minato-ku, Tokyo 108-8639; Departments of [2]Molecular Pathology and [3]Pathology, Graduate School of Biomedical Sciences, Hiroshima University, 1-2-3 Kasumi, Minami-Ku, Hiroshima 734-8551; [4]Department of Thoracic Surgery, Saitama Cancer Center, 818 Ina-machi, Kita-Adachi-gun, Saitama 362-0806; [5]Kanagawa Cancer Center Research Institute, 1-1-2 Nakao, Asahi-ku, Yokohama 241-0815, Japan

(Received July 17, 2007/Revised August 5, 2007/Accepted August 6, 2007/Online publication September 20, 2007)

To screen candidate molecules that might be useful as diagnostic biomarkers or for development of novel molecular-targeting therapies, we previously carried out gene-expression profile analysis of 101 lung carcinomas and detected an elevated expression of FGFR1OP (fibroblast growth factor receptor 1 oncogene partner) in the majority of lung cancers. Immunohistochemical staining using tumor tissue microarrays consisting of 372 archived non-small cell lung cancer (NSCLC) specimens revealed positive staining of FGFR1OP in 334 (89.8%) of 372 NSCLCs. We also found that the high level of FGFR1OP expression was significantly associated with shorter tumor-specific survival times ($P < 0.0001$ by log-rank test). Moreover, multivariate analysis determined that FGFR1OP was an independent prognostic factor for surgically treated NSCLC patients ($P < 0.0001$). Treatment of lung cancer cells, in which endogenous FGFR1OP was overexpressed, using FGFR1OP siRNA, suppressed its expression and resulted in inhibition of the cell growth. Furthermore, induction of FGFR1OP increased the cellular motility and growth-promoting activity of mammalian cells. To investigate its function, we searched for FGFR1OP-interacting proteins in lung cancer cells and identified ABL1 (Abelson murine leukemia viral oncogene homolog 1) and WRNIP1 (Werner helicase interacting protein 1), which was known to be involved in cell cycle progression. FGFR1OP significantly reduced ABL1-dependent phosphorylation of WRNIP1 and resulted in the promotion of cell cycle progression. Because our data imply that FGFR1OP is likely to play a significant role in lung cancer growth and progression, FGFR1OP should be useful as a prognostic biomarker and probably as a therapeutic target for lung cancer. (*Cancer Sci* 2007; 98: 1902–1913)

Lung cancer is the leading cause of cancer deaths worldwide, and non-small cell lung cancer (NSCLC) accounts for nearly 80% of those cases.[1] Many genetic alterations associated with development and progression of lung cancers have been reported, but the complex molecular mechanisms of pulmonary carcinogenesis remain largely unclear.[2] Systemic chemotherapy is the main treatment for the majority of patients with NSCLC, because most patients are diagnosed at an advanced stage of the disease. Within the last decade several newly developed cytotoxic agents such as paclitaxel, docetaxel, gemcitabine, and vinorelbine have begun to offer multiple choices for treatment of patients with advanced lung cancer; however, each of those regimens confers only a modest survival benefit compared with cisplatin-based therapies.[3,4] Hence, novel therapeutic strategies such as molecular-targeted drugs and antibodies, and cancer vaccines, are eagerly expected.

Systematic analysis of expression levels of thousands of genes using a cDNA microarray technology is an effective approach for identifying molecules involved in oncogenic pathways or those associated with efficacy of anticancer therapy; some of these genes or their gene products may be promising target molecules for the development of novel therapies and/or tumor biomarkers.[5–11] To identify such molecules, we established a new screening system consisting of the sequential steps of: (i) genome-wide expression profile analysis of 101 lung cancers (NSCLCs and SCLCs), coupled with enrichment of tumor cells by laser microdissection,[5–8,11] and its comparison with the data of the expression profile of 31 normal human tissues (27 adult and four fetal organs);[12,13] and (ii) verification of the biomedical and clinicopathological significance of the respective gene products by tumor-tissue microarray analysis of hundreds of archived lung-cancer materials, as well as RNA interference (RNAi) technologies.[14–27] This systematic approach revealed that the gene encoding fibroblast growth factor receptor 1 oncogene partner (FGFR1OP alias FOP) was overexpressed in the great majority of primary NSCLCs.

FGFR1OP was originally identified as a fusion partner for FGFR1 in the t(6;8)(q27;p11) chromosomal translocations in myeloproliferative disorders (MSD).[28–30] However, the biological roles of FGFR1OP during lung carcinogenesis have not been clarified. Werner helicase interacting protein 1 (WRNIP1 alias WHIP) was known to physically interact with WRN (Werner syndrome) protein that encodes a member of the RecQ subfamily and the DEAH (Asp-Glu-Ala-His) subfamily of DNA and RNA helicases.[31] WRNIP1 shows homology to replication factor C family proteins, and is conserved from *Escherichia coli* to humans.[32] Studies in yeast and human cells suggest that this gene may affect the aging process and interact with the DNA replication machinery to modulate the function of DNA polymerase δ (POLD) during DNA replication or replication-associated repair.[31,33–35] However, the roles of WRNIP1 in tumorigenesis are also uninvestigated.

In this study, we describe that overexpression of FGFR1OP could contribute to the malignant nature of lung cancer cells and that FGFR1OP significantly reduces ABL1-dependent phosphorylation of WRNIP1 and appears to promote cancer cell cycle progression. We suggest that targeting the FGFR1OP molecule might hold promise for the development of a new diagnostic and therapeutic strategy in the clinical management of lung cancers.

Materials and Methods

Cell lines and clinical tissue samples. Twenty-two human lung-cancer cell lines used in this study were as follows: 18 NSCLC cell lines, A427, A549, LC176, LC319, PC-9, PC-14, NCI-H520, NCI-H522, NCI-H647, NCI-H1373, NCI-H1666,

[6]To whom correspondence should be addressed. E-mail: yusuke@ims.u-tokyo.ac.jp

doi: 10.1111/j.1349-7006.2007.00610.x

NCI-H1703, NCI-H2170, RERF-LC-AI, SK-MES-1, SK-LU-1, LU61, and LX1, and four SCLC cell lines, DMS114, DMS273, SBC-3, and SBC-5. All cells were grown in monolayers in appropriate medium supplemented with 10% fetal calf serum (FCS) and maintained at 37°C in an atmosphere of humidified air with 5% CO_2. Human small airway epithelial cells (SAEC) were grown in optimized medium (SAGM) purchased from Cambrex Bio Science Inc. (Walkersville, MD). Surgically resected primary NSCLC samples had been obtained earlier with written informed consent. A total of 372 formalin-fixed samples of primary NSCLCs including 237 adenocarcinomas (ADCs), 94 squamous cell carcinoma (SCCs), 28 large cell carcinomas (LCCs), 13 adenosquamous carcinomas (ASCs) and adjacent normal lung tissues, had been obtained earlier along with clinicopathological data from patients who had a curative surgical operation at Saitama Cancer Center (Saitama, Japan). Lung cancer specimens and five adult tissues (heart, liver, lung, kidney, and testis) from postmortem materials (two individuals with NSCLC) had been obtained earlier at Hiroshima University (Hiroshima, Japan). The histological classification of the tumor specimens was carried out by the WHO criteria.[36] This study and the use of all clinical materials were approved by the Institutional Research Ethics Committees.

Semiquantitative RT-PCR analysis. Total RNA was extracted from cultured cells and clinical tissues using Trizol reagent (Life Technologies, Inc. Gaithersburg, MD) according to the manufacturer's protocol. Extracted RNAs and normal human-tissue polyA RNAs were treated with DNase I (Roche Diagnostics, Basel, Switzerland) and then reversely transcribed using oligo $(dT)_{12–18}$ primer and SuperScript II reverse transcriptase (Life Technologies). Semiquantitative reverse transcription-polymerase chain reaction (RT-PCR) experiments were carried out with synthesized *FGFR1OP* gene-specific primers (5′-CTGCTGGTACGTGTGATCTTTG-3′ and 5′-ACCTTAATG-GTCTAACAAACCTTCC-3′), or with β-actin (*ACTB*)-specific primers (5′-ATCAAGATCATTGCTCCTCCT-3′ and 5′-CTG-CGCAAGTTAGGTTTTGT-3′). PCR reactions were optimized for the number of cycles to ensure product intensity within the logarithmic phase of amplification.

Northern-blot analysis. Human multiple-tissue blot (23 normal tissues including heart, brain, placenta, lung, liver, skeletal muscle, kidney, pancreas, spleen, thymus, prostate, testis, ovary, small intestine, colon, peripheral blood leukocyte, stomach, thyroid, spinal cord, lymph node, trachea, adrenal gland, and bone marrow; BD Biosciences Clontech, Palo Alto, CA) was hybridized with a ^{32}P-labeled PCR product of *FGFR1OP*. The cDNA probes of *FGFR1OP* were prepared by RT-PCR using primers, 5′-TAAT-AGTACCAGCCATCGCTCAG-3′ and 5′-ATCCTACGGCTTT-ATTGACACCT-3′. Pre-hybridization, hybridization, and washing were carried out according to the supplier's recommendations. The blots were autoradiographed with intensifying screens at –80°C for one week.

Preparation of anti-FGFR1OP polyclonal antibody. Rabbit antibodies specific to FGFR1OP were raised by immunizing rabbits with histidine-tagged human FGFR1OP protein (codons 7–173; accession No. NM_007045), and purified with standard protocols using affinity columns (Affi-gel 10; Bio-Rad Laboratories, Hercules, CA) conjugated with the histidine-tagged protein. On Western blots we confirmed that the antibody was specific to FGFR1OP, using lysates from NSCLC tissues and cell lines as well as normal lung tissues.

Western-blot analysis. Cells were lyzed with radioimmuno-precipitation (RIPA) buffer (50 mM Tris-HCl [pH 8.0], 150 mM NaCl, 1% NP-40, 0.5% deoxychorate-Na, 0.1% sodium dodecyl sulphate [SDS]) containing protease inhibitor (Protease Inhibitor Cocktail Set III; CALBIOCHEM). Protein samples or immunoprecipitates were separated by SDS-polyacrylamide gels and electroblotted onto Hybond-ECL nitrocellulose membranes (GE Healthcare Bio-sciences). Blots were incubated with a rabbit polyclonal anti-FGFR1OP antibody, a mouse monoclonal FGFR1OP antibody (Abnova Corporation), a rabbit polyclonal WRNIP1 antibody (Abcam), a rabbit polyclonal ABL1 antibody (Cell Signaling Technology), a mouse monoclonal β-actin (ACTB) antibody (Sigma), or a mouse monoclonal anti-c-Myc antibody (Santa Cruz). Antigen-antibody complexes were detected using secondary antibodies conjugated to horseradish peroxidase (GE Healthcare Bio-sciences). Protein bands were visualized by enhanced chemiluminescence (ECL) western blotting detection reagents (GE Healthcare Bio-sciences), as previously described.[20]

Immunofluorescence analysis. Cultured cells were fixed with ice-cold methanol : acetone for 10 min at –20°C and subsequently washed with phosphate-buffered saline (PBS) (–). Prior to the primary antibody reaction, fixed cells were covered with CAS-BLOCK (ZYMED Laboratories) for 10 min to block non-specific antibody binding. Then the cells were incubated with a mouse monoclonal FGFR1OP antibody (Abnova Corporation), a rabbit polyclonal anti-WRNIP1 (Abcam) and a rabbit polyclonal ABL1 antibody (Santa Cruz Biotechnology). Antibodies were stained with an antimouse secondary antibody conjugated to Alexa Fluor 488 (Molecular Probes) and an antirabbit secondary antibody conjugated to Alexa Fluor 594 (Molecular Probes). DNA was stained with 4′6′-diamidino-2-phenylindole dihydrochloride (DAPI). To determine the cell cycle-dependent localization of FGFR1OP, synchronization at the G1–S boundary was achieved with aphidicolin block. Cells were blocked with 1 μg/mL of aphidicolin (Sigma-Aldrich) for 24 h, and released from the block by four washes with PBS. These cells were cultured in medium and harvested for analysis at 1.5, 4.0 and 9.0 h after release from the cell-cycle arrest. Images were viewed and assessed using a confocal microscope at wavelengths of 488, 594 nm (TCS SP2 AOBS: Leica Microsystems).

Flow cytometry. Cells were trypsinized, collected in PBS and fixed in 70% cold ethanol for 30 min. After treatment with 100 μg/mL of RNase (Sigma-Aldrich), the cells were stained with 50 μg/mL of propidium iodide (Sigma-Aldrich) in PBS. Flow cytometry was carried out on a Becton Dickinson FACScan and analyzed with ModFit software (Verity Software House, Topsham, ME). The cells selected from at least 20 000 ungated cells were analyzed for DNA content.

Immunohistochemistry and tissue microarray. Tumor-tissue microarrays were constructed using 372 formalin-fixed primary NSCLCs, as published previously.[37–39] The tissue area for sampling was selected by visual alignment with the corresponding HE-stained section on a slide. Three, four, or five tissue cores (diameter 0.6 mm; height 3–4 mm) taken from a donor tumor block were placed into a recipient paraffin block using a tissue microarrayer (Beecher Instruments, Sun Prairie, WI). A core of normal tissue was punched from each case, and 5-μm sections of the resulting microarray block were used for immunohistochemical analysis.

To investigate the presence of FGFR1OP protein in clinical samples that had been embedded in paraffin blocks, we stained the sections as previously described.[18,20,25] Briefly, a rabbit polyclonal antihuman FGFR1OP antibody was added after blocking of endogenous peroxidase and proteins. The sections were incubated with HRP-labeled antirabbit IgG as the secondary antibody. Substrate-chromogen was added and the specimens were counterstained with hematoxylin.

Three independent investigators assessed FGFR1OP positivity semiquantitatively without prior knowledge of clinicopathological data. The intensity of FGFR1OP staining was evaluated using the following criteria: strong positive (2+), dark brown staining in more than 50% of tumor cells completely obscuring nucleus and cytoplasm; weak positive (1+), any lesser degree of brown staining appreciable in nucleus and cytoplasm; absent (scored as 0), no appreciable staining in tumor cells. Cases were accepted

only as strongly positive if the three reviewers independently defined them as such.

Statistical analysis. Statistical analyses were performed using the StatView statistical program (SaS, Cary, NC). We used contingency tables to analyze the relationship between FGFR1OP expression and clinicopathological variables in NSCLC patients. Tumor-specific survival curves were calculated from the date of surgery to the time of death related to NSCLC, or to the last follow-up observation. Kaplan-Meier curves were calculated for each relevant variable and for FGFR1OP expression; differences in survival times among patient subgroups were analyzed using the log-rank test. Univariate and multivariate analyses were carried out with the Cox proportional-hazard regression model to determine associations between clinicopathological variables and cancer-related mortality. First, we analyzed associations between death and possible prognostic factors including age, gender, histological type, pT-classification, pN-classification, and smoking history, taking into consideration one factor at a time. Second, multivariate Cox analysis was applied on backward (stepwise) procedures that always forced strong FGFR1OP expression into the model, along with any and all variables that satisfied an entry level of a P-value of less than 0.05. As the model continued to add factors, independent factors did not exceed an exit level of $P < 0.05$.

RNA interference assay. Using the vector-based RNA interference (RNAi) system, psiH1BX3.0, which we had established earlier to direct the synthesis of siRNAs in mammalian cells,[14] we transfected 10 μg of siRNA-expression vector with 30 μL of Lipofectamine 2000 (Invitrogen) into two lung-cancer cell lines, LC319 and SBC-5, that endogenously overexpressed FGFR1OP. The transfected cells were cultured for 5 days in the presence of appropriate concentrations of geneticin (G418). Cell numbers and viability were measured by Giemsa staining and 3-(4,5-dimethylthiazol-2-yl)-2,5-diphenyltetrazolium bromide (MTT) assay in triplicate. The target sequences of the synthetic oligonucleotides for RNAi were as follows: control-1 (EGFP, enhanced green fluorescent protein [GFP] gene, a mutant of *Aequorea victoria* GFP), 5′-GAAGCAGCACGACTTCTTC-3′; control-2 (LUC, luciferase gene from *Photinus pyralis*), 5′-CGTACGCGGAATACTTCGA-3′; control-3 (SCR, scramble chloroplast *Euglena gracilis* gene coding for the 5S and 16S rRNA), 5′-GCGCGCTTTGTAGGATTCG-3′; siRNA-FGFR1OP-1 (si-1), 5′-CCTGAAACTAGCACACTGC-3′; siRNA-FGFR1OP-2 (si-2), ′5-GGTAAGAAGAAGACAAGCG-3′. To validate our RNAi system, downregulation of *FGFR1OP* expression by functional siRNA, but not by controls, was confirmed in the cell lines used for this assay.

Cell migration assay. Using FuGENE 6 Transfection Reagent (Roche Diagnostics) according to the manufacturer's instructions, we transfected COS-7 cells with plasmids expressing FGFR1OP (pCDNA3.1/myc-His-FGFR1OP) or mock plasmids (pCDNA3.1/myc-His). Transfected cells were harvested and suspended in Dulbecco's modified Eagle's medium (DMEM) without FCS. DMEM containing 10% FCS was added to each lower chamber of 24-well migration chambers (Becton Dickinson Labware) and cell suspension was added to each insert of the upper chamber. The plates of inserts were incubated for 24 h at 37°C, then subsequently extracted and stained migrated-cells on the bottom side of the membrane.

Matrigel invasion assay. COS-7 cells transfected either with plasmids expressing FGFR1OP (pCDNA3.1/myc-His-FGFR1OP) or with mock plasmids were grown to near confluence in DMEM containing 10% FCS. The cells were harvested by trypsinization, washed in DMEM without addition of serum or proteinase inhibitor, and suspended in DMEM at concentration of 1×10^5 cells/mL. Before preparing the cell suspension, the dried layer of Matrigel matrix (Becton Dickinson Labware) was rehydrated with DMEM for 2 h at room temperature. DMEM (0.75 mL) containing 10% FCS was added to each lower chamber in 24-well Matrigel invasion chambers, and 0.5 mL (5×10^4 cells) of the cell suspension was added to each insert of the upper chamber. The plates of inserts were incubated for 22 h at 37°C and the chambers were processed; cells invading through the Matrigel were fixed and stained by Giemsa as directed by the supplier (Becton Dickinson Labware).

Identification of FGFR1OP-associated proteins. Cell extracts from lung-cancer cell line LC319 were precleared by incubation at 4°C for 1 h with 100 μL of protein G-agarose beads in a final volume of 2 mL of immunoprecipitation buffer (0.5% NP-40, 50 mM Tris-HCl, 150 mM NaCl) in the presence of proteinase inhibitor. After centrifugation at 80g for 5 min at 4°C, the supernatant was incubated at 4°C with anti-FGFR1OP polyclonal antibody or normal rabbit IgG for 2 h. The beads were then collected by centrifugation at 2000g for 2 min and washed six times with 1 mL of each immunoprecipitation buffer. The washed beads were resuspended in 50 μL of Laemmli sample buffer and boiled for 5 min, and the proteins were separated in 5–20% SDS polyacrylamide gel electrophoresis (PAGE) gels (BIO RAD). After electrophoresis, the gels were stained with silver. Protein bands specifically found in extracts immunoprecipitated with anti-FGFR1OP polyclonal antibody were excised and served for matrix-assisted laser desorption/ionization-time of flight mass spectrometry (MALDI-TOF-MS) analysis (AXIMA-CFR plus, SHIMADZU BIOTECH).

ABL1 kinase assay. Recombinant FGFR1OP (Abnova Corporation) and WRNIP1 were immunoprecipitated with anti-c-myc antibodies using cell extracts from COS-7 cells transfected with plasmids expressing myc-tagged proteins (pCDNA3.1/myc-His-FGFR1OP or pCDNA3.1/myc-His-WRNIP1). Full-length human recombinant His-tagged ABL1 (Invitrogen) was incubated with the recombinant FGFR1OP or WRNIP1 in kinase assay buffer (50 mM Tris, pH 7.4, 10 mM $MgCl_2$, 2 mM dithiothreitol, 1 mM NaF, 0.2 mM ATP) for 60 min at 30°C. The reactions were terminated by the addition of Laemmli sample buffer and heating at 95°C for 5 min. We detected *in vitro* phosphorylated samples by standard SDS-PAGE and subsequent western-blotting using anti-pan-phosphotyrosine antibodies or [γ-^{32}P]-ATP incorporation assays, as reported previously.[26]

BrdU-incorporation assay. Lung-cancer A549 cells transfected with plasmids designed to express ABL1 (pCDNA3.1/myc-His-ABL1), FGFR1OP (pCDNA3.1/myc-His-FGFR1OP), or WRNIP1 (pCDNA3.1/myc-His-WRNIP1), or mock plasmids (pCDNA3.1/myc-His), were cultured for 48 h. BrdU (5-bromodeoxyuridine) solution was then added in culture medium, and the cells were incubated for 8 h and fixed; incorporated BrdU was measured using a commercially available kit (Cell Proliferation ELISA, BrdU; Roche Diagnostics, Basel, Switzerland).

Results

FGFR1OP expression in lung tumors and normal tissues. To identify target molecules for the development of novel therapeutic agents and/or biomarkers for lung cancer, we first screened a cDNA microarray consisting 27 648 genes, and found the *FGFR1OP* transcript to be overexpressed in the majority of lung cancer samples examined. We then confirmed its transactivation by semiquantitative RT-PCR experiments in nine of 14 additional NSCLC tissues and in 17 of 19 lung-cancer cell lines (Fig. 1a). Because FGFR1OP was originally identified as a fusion partner for FGFR1 in t(6;8)(q27;p11) chromosomal translocations responsible for myeloproliferative disorders (MSD), we screened *FGFR1-FGFR1OP* fusion transcripts in various lung-cancer cell lines using *FGFR1OP* and *FGFR1* specific primers.[28–30] Both *FGFR1OP* and *FGFR1* transcripts were detected in all lung-cancer cell lines examined, but neither *FGFR1OP-FGFR1* nor *FGFR1-FGFR1OP* reciprocal transcripts was detected (data not shown).

doi: 10.1111/j.1349-7006.2007.00610.x

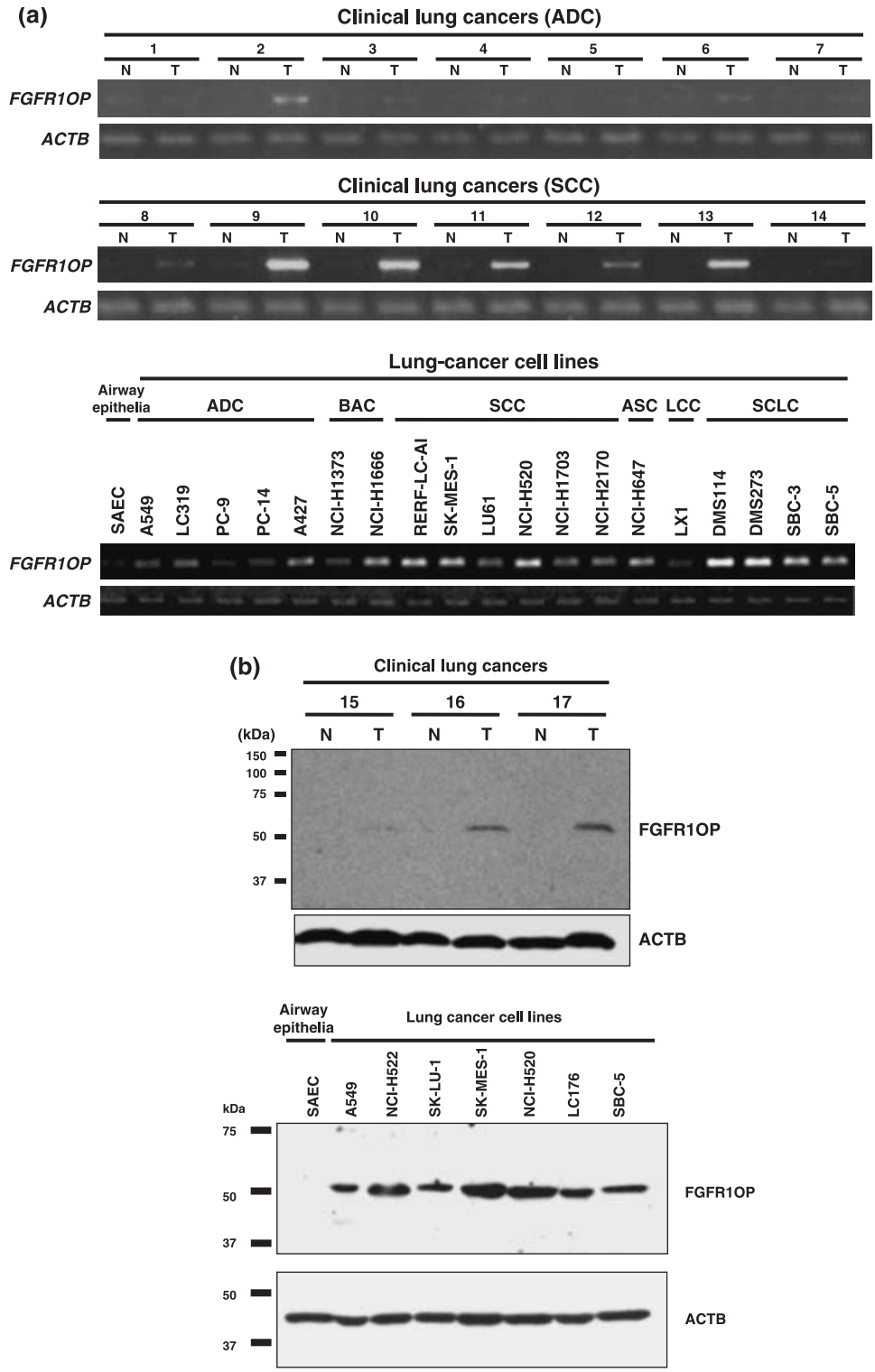

Fig. 1. Fibroblast growth factor receptor 1 oncogene partner (FGFR1OP) expression in lung cancers and normal tissues. (a) Expression of *FGFR1OP* in clinical samples of non-small cell lung cancer (NSCLC) (T) and corresponding normal lung tissues (N), examined by semiquantitative reverse transcription-polymerase chain reaction (RT-PCR) (upper panels). Expression of *FGFR1OP* in lung-cancer cell lines, detected by semiquantitative RT-PCR (lower panels). (b) Western-blot analysis of FGFR1OP protein in three representative pairs of lung-cancer tissue samples (upper panels). Western-blot analysis of FGFR1OP protein in lung-cancer cell lines (lower panels). (c) Cell-cycle dependent localization of endogenous FGFR1OP. LC319 cells were synchronized at the G1/S boundary by aphidicolin. At different time-points after the release from cell-cycle arrest, fluorescence-activated cell sorting (FACS) analysis, immunocytochemical staining was carried out. Cells were immunostained with FGFR1OP-Alexa488 (green) using anti-FGFR1OP antibody or cell nuclei (blue; 4′6′-diamidino-2-phenylindole dihydrochloride [DAPI]) at individual time points. (d) Upper panel, Northern-blot analysis of the FGFR1OP transcript in 23 normal adult human tissues. Lower panels, immunohistochemical evaluation of FGFR1OP protein in representative normal tissues and lung cancers; adult heart, liver, lung, kidney, testis and lung adenocarcinoma tissue. Magnification, ×200.

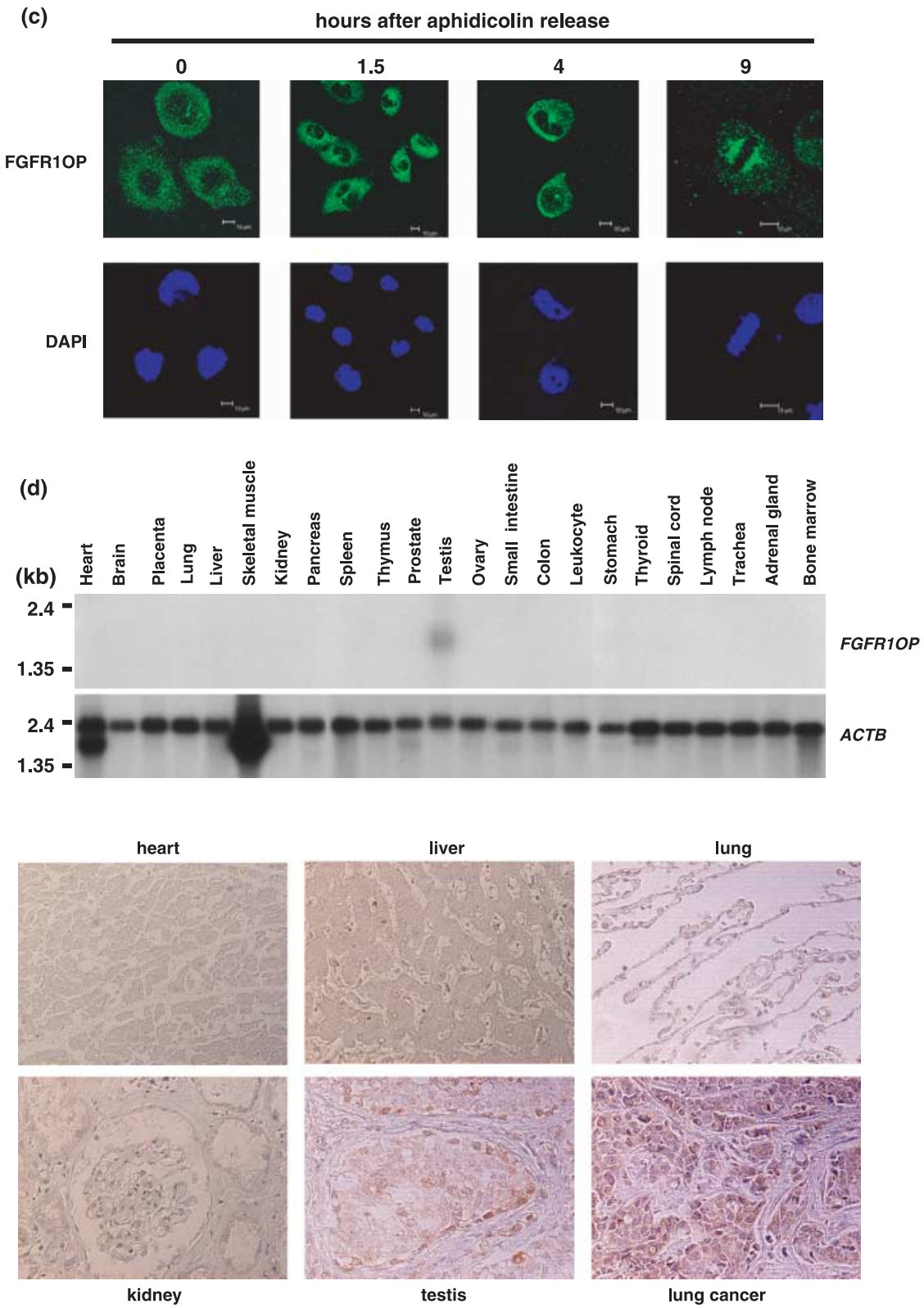

Fig. 1. *Continued*

We subsequently examined by western-blot analysis an expression of FGFR1OP protein in lung cancer tissues and cell lines, and found the increased FGFR1OP protein expression in representative pairs of clinical lung cancer tissue samples and in lung-cancer cell lines (Fig. 1b). We then carried out immunofluorescence analysis to examine the subcellular localization of endogenous FGFR1OP in lung-cancer cells. LC319 cells, synchronized using aphidicolin, were harvested for flow cytometric and immunofluorescence analyses at various time-points after release from the cell-cycle arrest. Before removal of aphidicolin

doi: 10.1111/j.1349-7006.2007.00610.x

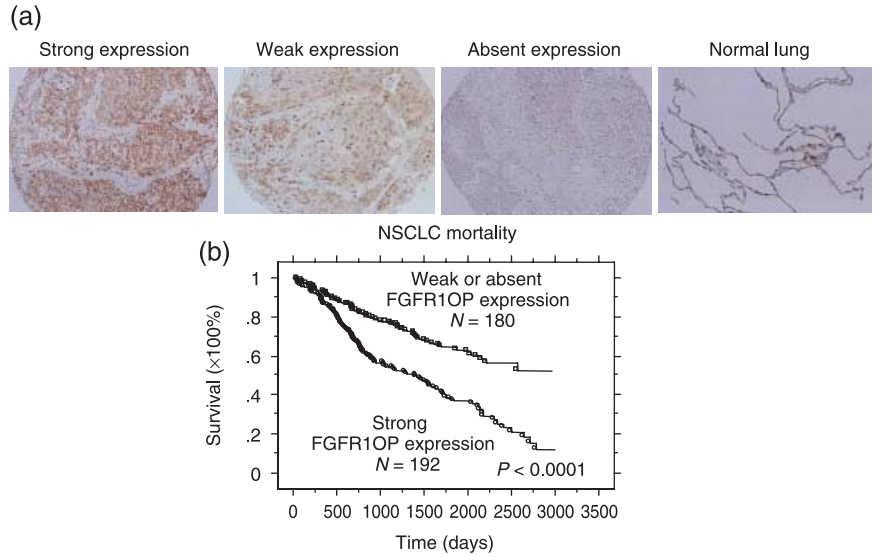

Fig. 2. Fibroblast growth factor receptor 1 oncogene partner (FGFR1OP) protein expression and its association with poorer clinical outcomes for non-small cell lung cancer (NSCLC) patients. (a) Immunohistochemical evaluation of FGFR1OP protein expression on tissue microarrays. Examples are shown for strong, weak, or absent FGFR1OP expression in lung squamous cell carcinomas, and for no expression in normal lung. Magnification, ×100. (b) Kaplan-Meier analysis of tumor-specific survival in 372 patients with NSCLCs according to the level of FGFR1OP expression ($P < 0.0001$; log-rank test).

(0 h), FGFR1OP was observed in nucleus and cytoplasm with granular appearance. At 1.5 h after release when most cells were in the S phase, FGFR1OP was stained in nucleus and cytoplasm as well as centrosome. Interestingly, FGFR1OP was detected mainly in perinucleus as well as in nucleus at 4 h when the cells started to enter the G2/M phase. At 9 h, when most cells were in the G2/M phase, FGFR1OP was localized mainly in centrosome and cytoplasm (Fig. 1c). FGFR1OP protein levels were not changed during cell cycle progression, as detected by western-blot analysis (data not shown).

Northern blot analysis using an *FGFR1OP* cDNA fragment as a probe identified a transcript of about 1.8 kb that was expressed only in the testis among 23 normal human tissues examined (Fig. 1d, upper panels). We subsequently examined the expression of FGFR1OP protein with the anti-FGFR1OP antibody on five normal tissues (heart, liver, lung, kidney, and testis) and NSCLC tissues, and found that positive staining was observed in cytoplasm and/or nucleus of primary lung cancer cells and testicular cells (Fig. 1d, lower panels).

Association of FGFR1OP overexpression with poor clinical outcome for NSCLC patients. To verify the biological and clinicopathological significance of FGFR1OP, we also examined the expression of FGFR1OP protein by means of tissue microarrays containing 372 primary NSCLC tissues (Fig. 2a). We classified a pattern of FGFR1OP expression on the tissue array into three classes, absent (scored as 0), weak positive (scored as 1+), and strong positive (scored as 2+). Positive staining (scored 2+ and 1+) was observed in 206 (86.9%) of 237 ADC cases examined, in 92 (97.9%) of 94 SCCs, in 24 (85.7%) of 28 LCCs and in 12 (92.3%) of 13 ASCs, while no staining was observed in any of the normal portions of the same tissues. Strong FGFR1OP expression (scored 2+) was observed in 116 (48.9%) of 237 ADC cases examined, 54 (57.4%) of 94 SCCs, 12 (42.9%) of 28 LCCs and 10 (76.9%) of 13 ASCs. We evaluated the association between FGFR1OP status and clinicopathological variables among surgically resected lung cancers, and found that tumor size (pT2-4 *versus* pT1; $P = 0.0031$ by Fisher's exact test) and lymph node metastasis (pN1-2 *versus* pN0; $P = 0.0056$ by Fisher's exact test) were significantly associated with the strong FGFR1OP expression (Table 1). The median survival time of patients with strong FGFR1OP-staining tumors (scored 2+) was significantly shorter than that of patients with absent and/or weak FGFR1OP-staining (scored 0 and 1+) ($P < 0.0001$ by log-rank test; Fig. 2b). We also used univariate analysis to evaluate associations between patient prognosis and other factors including age (≥65 *vs* <65), gender (male *vs* female), histological classification (other histological types *vs* adenocarcinoma), pT classification (pT2-4 *vs* pT1) and pN classification (pN1–2 *vs* pN0), smoking history (current and former smoker *vs* never-smoker), and FGFR1OP status (scored 2+ *vs* scored 0, 1+) (Table 2). Among those parameters, strong FGFR1OP expression ($P < 0.0001$), elderly ($P = 0.0375$), male gender ($P = 0.0008$), non-adenocarcinoma histological type ($P = 0.009$), advanced pT stage ($P < 0.0001$), and advanced pN stage ($P < 0.0001$) were significantly associated with poor prognosis. In multivariate analyses of prognostic factors, strong FGFR1OP expression ($P < 0.0001$) as well as elderly ($P = 0.0036$), advanced pT stage ($P = 0.0009$), and advanced pN stage ($P < 0.0001$) were significant and independent unfavorable prognostic factors (Table 2).

Effect of FGFR1OP on cell growth. To assess whether upregulation of FGFR1OP plays a role in growth or survival of lung-cancer cells, we constructed plasmids to express siRNA against *FGFR1OP* (si-1 and -2), along with three different control plasmids (siRNAs for EGFP, LUC, and SCR), and transfected them into LC319 and SBC-5 cells to suppress expression of endogenous *FGFR1OP* (Fig. 3a). The level of *FGFR1OP* expression in the cells transfected with si-1 was significantly reduced, in comparison with those with any of the three control siRNAs (Fig. 3a, upper panels). si-2 showed almost no suppressive effect on *FGFR1OP* expression. Cell viability and colony numbers measured by MTT and colony-formation assays were reduced significantly in the cells transfected with si-1 in comparison with those transfected with the other plasmid clones (Fig. 3a, lower panels).

To further examine a potential role of FGFR1OP in tumorigenesis, we prepared plasmids designed to express FGFR1OP (pcDNA3.1/myc-His-FGFR1OP) and transfected them into COS-7 cells. After confirmation of FGFR1OP expression by western-blot analysis (Fig. 3b, left panels), we carried out MTT and colony-formation assays, and found that growth of the FGFR1OP-COS-7 cells was promoted at a significant degree in comparison to the COS-7 cells transfected with the mock vector (Fig. 3b, right upper and lower panels). There was also a remarkable tendency in the COS-7-FGFR1OP cells to form larger colonies than the control cells (Fig. 3b, right lower panels), implying that FGFR1OP has an oncogenic activity in mammalian cells.

Activation of cellular migration and invasion by FGFR1OP. As the immunohistochemical analysis on tissue microarray indicated that lung cancer patients with FGFR1OP strong-positive tumors showed a shorter cancer-specific survival period than those with FGFR1OP-weak-positive and/or negative tumors, we examined a

Table 1. Association between FGFR1OP-positivity in NSCLC tissues and patients' characteristics (n = 372)

	Total (n = 372)	FGFR1OP strong expression (n = 192)	FGFR1OP weak expression (n = 142)	FGFR1OP absent expression (n = 38)	P-value strong positive *vs* weak/absent
Sex					
Male	258	141	93	24	NS
Female	114	51	49	14	
Age (years)					
<65	186	103	63	20	NS
≥65	186	89	79	18	
Histological type					
ADC	237	116	90	31	NS‡
SCC	94	54	38	2	
Others†	41	22	14	5	
pT factor					
T1	125	51	53	21	0.0031*
T2–4	247	141	89	17	
pN factor					
N0	229	105	95	29	0.0056*
N1 + N2	143	87	47	9	
Smoking history					
Never smoker	113	57	43	13	NS
Smoker	259	135	99	25	

*P < 0.05 (Fisher's exact test). †Large cell carcinoma (LCC) plus adenosquamous cell carcinoma (ASC). ‡ADC versus non-ADC (SCC and others). ADC, adenocarcinoma; NS, no significance; SCC, squamous cell carcinoma.

Table 2. Cox's proportional hazards model analysis of prognostic factors in NSCLC patients

Variables	Hazards ratio	95% CI	Unfavorable/favorable	P-value
Univariate analysis				
FGFR1OP	2.236	1.656–3.020	Strong (+)/weak (+) or (–)	<0.0001*
Age (years)	1.358	1.018–1.812	≥65/<65	0.0375*
Sex	1.776	1.270–2.484	Male/female	0.0008*
Histological type	1.470	1.101–1.962	non-ADC/ADC1	0.0090*
pT factor	2.639	1.848–3.784	T2–T4/T1	<0.0001*
pN factor	2.569	1.927–3.423	N1 + N2/N0	<0.0001*
Smoking history	1.276	0.927–1.756	smoker/non-smoker	NS
Multivariate analysis				
FGFR1OP	1.892	1.396–2.564	Strong (+)/weak (+) or (–)	<0.0001*
Age (years)	1.552	1.155–2.086	≥65/<65	0.0036*
Sex	1.382	0.955–2.000	Male/female	NS
Histological type	1.091	0.796–1.493	non-ADC/ADC	NS
pT factor	1.885	1.295–2.744	T2–4/T1	0.0009*
pN factor	2.380	1.769–3.201	N1 + N2/N0	<0.0001*

*P < 0.05. ADC, adenocarcinoma; NS, no significance.

possible role of FGFR1OP in cellular migration and invasion using cell migration and Matrigel invasion assays. Transfection of FGFR1OP-expressing plasmids (pcDNA3.1/myc-His-FGFR1OP) into COS-7 cells significantly enhanced its migration as well as invasive activity through Matrigel, compared to cells transfected with mock vector (Fig. 3c,d).

Identification of molecules interacting with FGFR1OP. To elucidate the biological mechanism of FGFR1OP in lung carcinogenesis, we attempted to identify proteins that would interact with FGFR1OP in lung cancer cells. Cell extracts from LC319 cells were immunoprecipitated with anti-FGFR1OP antibody or rabbit IgG (negative control). Following separation by SDS-PAGE, protein complexes were silver-stained. Protein bands, which were seen in immunoprecipitates by anti-FGFR1OP antibody, but not in those by rabbit IgG, were excised, trypsin-digested, and subjected to mass spectrometry analysis. Peptides from two independent protein bands matched to amino-acid sequences of WRNIP1 and ABL1. We subsequently confirmed the cognate interaction of endogenous FGFR1OP with endogenous WRNIP1 or ABL1 in LC319 cells by immunoprecipitation experiments (Fig. 4a).

***In vitro* and *in vivo* phosphorylation of WRNIP1 by ABL1.** Since ABL1 is a latent tyrosine kinase that could regulate many cellular processes including inhibition of the cell cycle progression,[40,41] we examined whether FGFR1OP or WRNIP1 could be a potential substrate for ABL1. We carried out an *in vitro* kinase assay by incubating recombinant His-tagged ABL1 protein with c-myc tagged FGFR1OP or c-myc-tagged WRNIP1 (Fig. 4b,c). Subsequent western-blot analysis using anti-pan-phosphotyrosine specific antibodies detected that WRNIP1 was phosphorylated by ABL1 tyrosine kinase (Fig. 4b, right panels), whereas there was no detectable ABL1-dependent phosphorylation of FGFR1OP (Fig. 4b, left panels). We confirmed the phosphorylation of WRNIP1 using the same assay in the presence of

doi: 10.1111/j.1349-7006.2007.00610.x

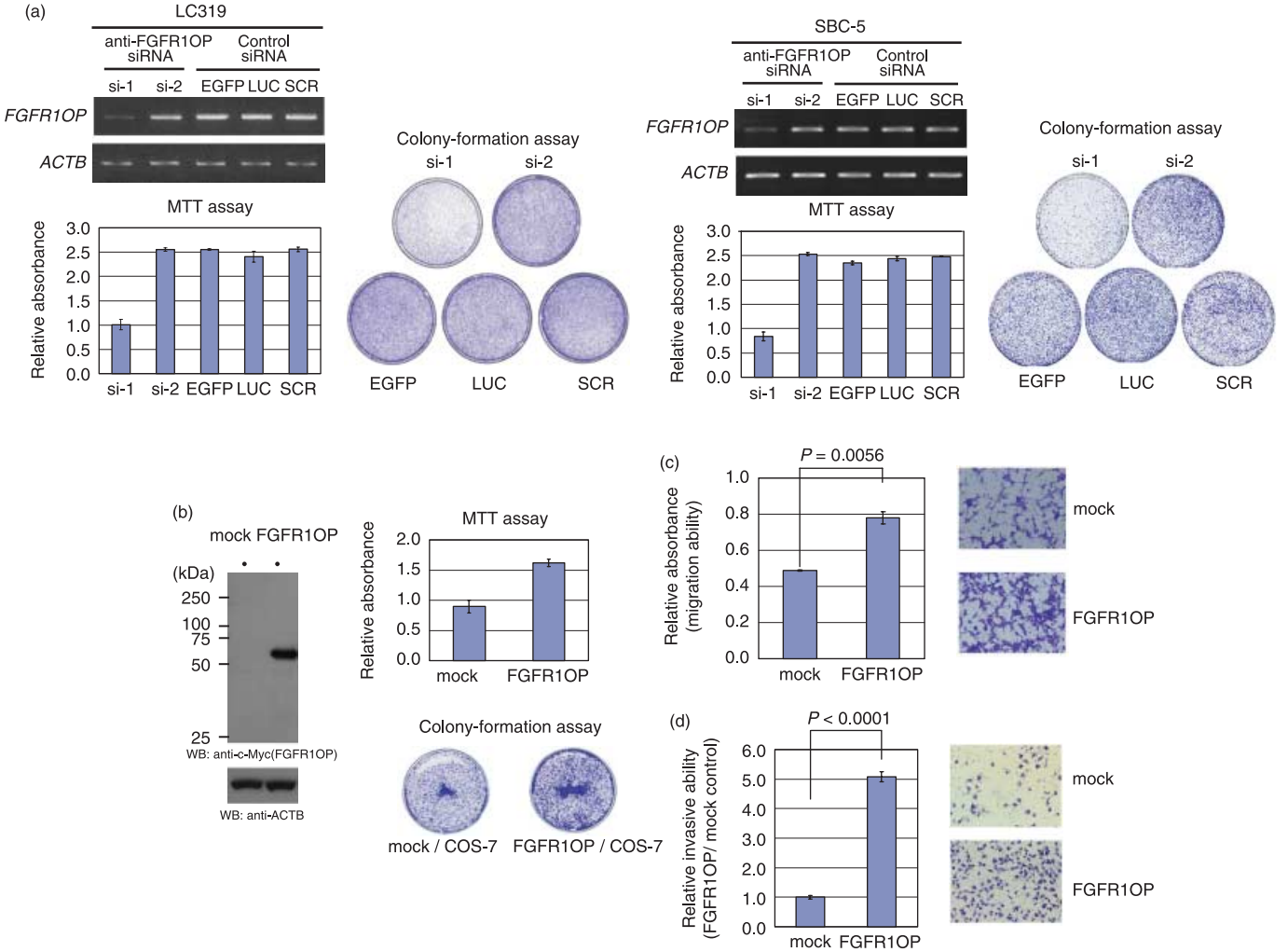

Fig. 3. Effect of fibroblast growth factor receptor 1 oncogene partner (FGFR1OP) on growth and invasive activity of cells. (a) Expression of *FGFR1OP* in response to si-FGFR1OPs (si-1 and -2) or control siRNAs (EGFP, enhanced green fluorescent protein [GFP], luciferase [LUC], or scramble [SCR]) in LC319 (left) and SBC-5 (right) cells, analyzed by semiquantitative reverse transcription-polymerase chain reaction (RT-PCR) (upper panels). Viability of LC319 or SBC-5 cells evaluated by MTT assay in response to si-1, si-2, si-EGFP, si-LUC, or si-SCR (lower panels). Colony-formation assays of LC319 and SBC-5 cells transfected with specific siRNAs or control plasmids (lower panels). All experiments were carried out in triplicate. (b) Effect of FGFR1OP on growth of COS-7 cells. Expression of FGFR1OP in COS-7 cells examined by western-blot analysis (left panels). The cells transfected with pcDNA3.1-myc-His-FGFR1OP or mock vector were each cultured in triplicate, the cell viability was evaluated by the MTT assay (right upper panel). Sizes and numbers of colonies derived from cells transfected with FGFR1OP-expressing plasmids are greater than those with mock vector (right lower panels). (c) Cell migration assay demonstrating the increased motility of COS-7 cells transfected with expression plasmids for FGFR1OP. Colorimetric measurements and Giemsa staining were shown (×200) (left and right panels). Assays were carried out three times, and each in triplicate wells. (d) Assays demonstrating the invasive nature of COS-7 cells in Matrigel matrix after transfection with expression plasmids for FGFR1OP. Giemsa staining (×200) and the number of cells migrating through the Matrigel-coated filters (left and right panels). Assays were carried out three times, and each in triplicate wells.

[γ-^{32}P]-ATP (Fig. 4c). To further examine whether WRNIP1 could be phosphorylated by ABL1 *in vivo*, we exogenously overexpressed both c-myc-tagged WRNIP1 and Flag-tagged ABL1 in COS-7 cells, and subsequently immunoprecipitated the WRNIP1 with anti-c-myc antibody and immunoblotted it using anti-pan-phosphotyrosine antibody. Expectedly, tyrosine phosphorylation of WRNIP1 by ABL1 was detected (Fig. 4d). These data suggested that WRNIP1 was likely to be a cognate substrate of ABL1 kinase.

Inhibition of ABL1-dependent phosphorylation of WRNIP1 by FGFR1OP. To elucidate the function of the interaction between FGFR1OP and WRNIP1/ABL1 in lung carcinogenesis, we examined the subcellular localization of these proteins in lung cancer cells, A549. Immunocytochemical analysis using anti-FGFR1OP and anti-WRNIP1/ABL1 antibodies demonstrated that endogenous FGFR1OP was colocalized with endogenous WRNIP1 and ABL1 mainly in perinucleus as well as in nucleus at S ~ G2/M phase (Fig. 5a).

To determine whether FGFR1OP could affect phosphorylation of WRNIP1 by ABL1, we carried out *in vitro* kinase assay by incubating c-myc tagged WRNIP1 with His-tagged ABL1 in the absence or presence of recombinant glutathione-S-transferase (GST)-tagged FGFR1OP. As shown in Fig. 5b, FGFR1OP significantly inhibited the ABL1 kinase activity on WRNIP1 in a dose-dependent manner. We then examined the effect of FGFR1OP overexpression on ABL1-induced cell cycle arrest. We measured the BrdU incorporation ability of A549 cells that were overexpressed either ABL1, or both ABL1 and FGFR1OP, and found that ABL1-induced cell cycle arrest was recovered by overexpression of FGFR1OP (Fig. 5c). These results suggested that FGFR1OP might block phosphorylation of WRNIP1 by ABL1 and play a significant role in pulmonary carcinogenesis.

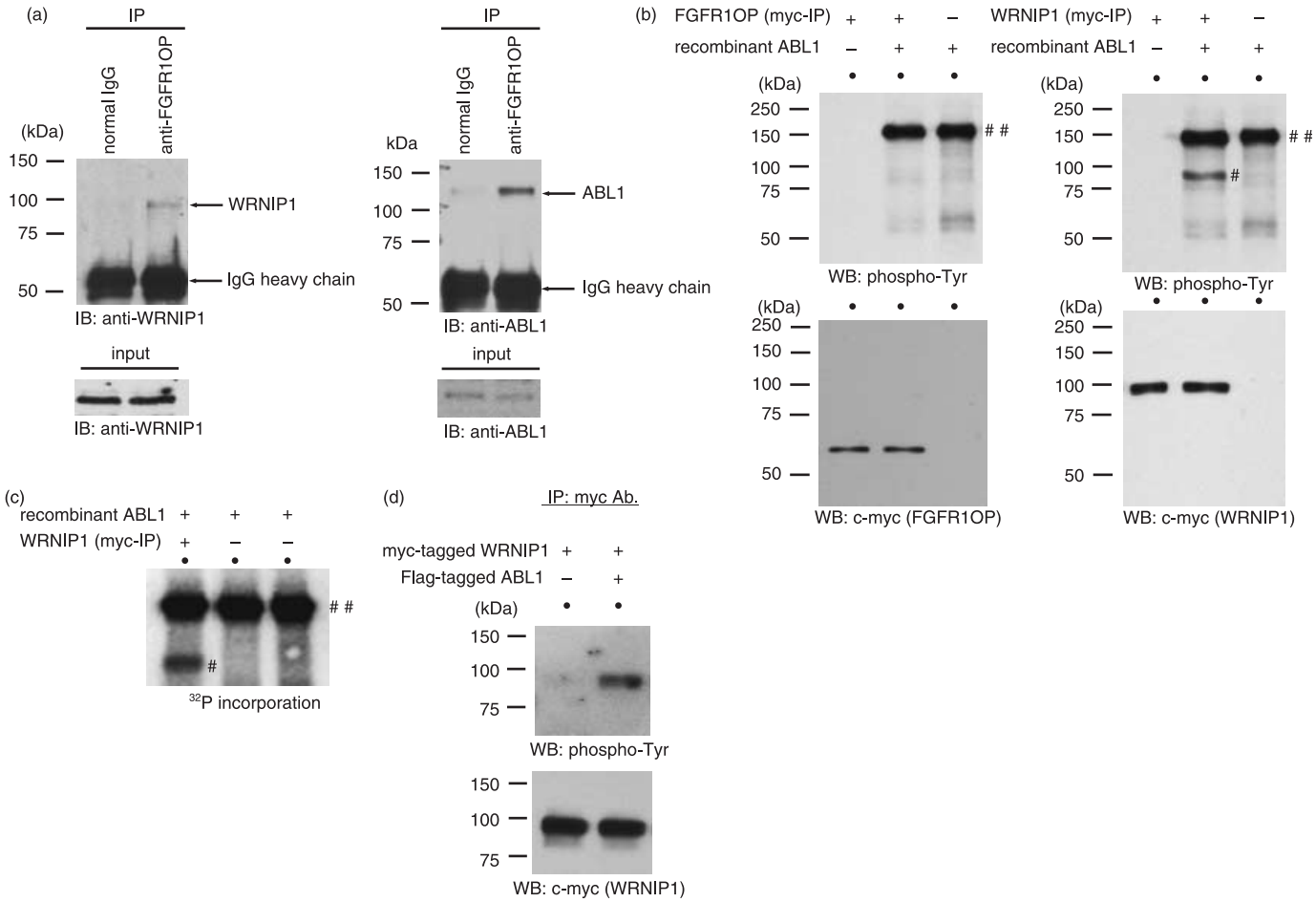

Fig. 4. Interaction of fibroblast growth factor receptor 1 oncogene partner (FGFR1OP) with novel FGFR1OP-binding proteins. (a) Interaction of endogenous FGFR1OP with Werner helicase interacting protein 1 (WRNIP1) and ABL1 in lung cancer cells. Immunoprecipitations were carried out using anti-FGFR1OP antibodies and extracts from LC319 cells. Immunoprecipitates were subjected to western-blot analysis to detect endogenous WRNIP1 (left panels) or ABL1 (right panels). IB, immunoblotting; IP, immunoprecipitation. (b) ABL1 kinase assays, conducted by incubating c-myc-tagged FGFR1OP (left panels; anti-c-myc immunoprecipitates from COS-7 cells transfected with expression plasmids for c-myc-tagged FGFR1OP) or c-myc-tagged WRN1IP (right panels; antic-myc immunoprecipitates from COS-7 cells transfected with expression plasmids for c-myc-tagged WRNIP1) with recombinant ABL1 (as kinase). After the kinase reaction, samples were subjected to western-blot analysis with anti-pan-phosphotyrosine antibodies. The phosphorylated form of WRNIP1 by recombinant ABL1 (#) and the autophosphorylated form of recombinant ABL1 (##) were indicated. (c) c-myc-tagged WRN1IP was incubated with recombinant ABL1 and [γ-^{32}P]-ATP. The reaction samples were analyzed by sodium dodecyl sulfate-polyacrylamide gel electrophoresis (SDS-PAGE) and autoradiography. The phosphorylated form of WRNIP1 by recombinant ABL1 (#) and the autophosphorylated form of recombinant ABL1 (##) were indicated. (d) COS-7 cells were cotransfected with expression plasmids for c-myc-tagged WRNIP1 and expression plasmids for Flag-tagged ABL1 or empty plasmids. The anti-c-myc immunoprecipitates (c-myc-tagged WRNIP1) were subjected to western-blot analysis with anti-pan-phosphotyrosine antibodies.

To further assess whether expression of WRNIP1 plays a role in growth of lung-cancer cells, we then examined the biological significance of the WRNIP1 function in pulmonary carcinogenesis using siRNAs against *WRNIP1* (si-*WRNIP1*-#1 and -#2). Treatment of LC319 cells with siRNA oligonucleotides against WRNIP1 (si-*WRNIP1*-1 or -2) suppressed expression of the endogenous *WRNIP1* in comparison to the control siRNAs (Fig. 5d, left upper panels). In accordance with the reduced expression of *WRNIP1*, LC319 cells showed significant decreases in cell viability and numbers of colonies (Fig. 5d, left lower and right panels). These results strongly supported the possibility that WRNIP1 might also play a significant role in growth and/or survival of lung cancer cells.

Discussion

Molecular-targeted therapies are expected to be highly specific to malignant cells, with minimal risk of adverse reactions due to their well-defined mechanisms of action. Equally desirable prospects are minimally invasive, and highly sensitive and specific new diagnostic methods using selected biomarkers that would adapt readily to clinical settings. As an approach to this goal, we have undertaken a strategy that combines screening of candidate molecules by genome-wide expression analysis with high-throughput screening of loss-of-function effects, using the RNAi technique. In addition, we have been using the tissue-microarray method to analyze hundreds of archived clinical samples for validation of potential target proteins. Using this combined approach, we have shown here that FGFR1OP is frequently overexpressed in clinical lung-cancer samples, and cell lines, and that the gene product plays indispensable roles in the growth and progression of lung-cancer cells.

FGFR1OP protein encodes a 399-amino-acid protein with a LisH domain. LisH motifs in some proteins are reported to be involved in microtubule dynamics and organization, cell migration, and chromosome segmentation.[42,43] A t(6;8)(q27;p11)

doi: 10.1111/j.1349-7006.2007.00610.x

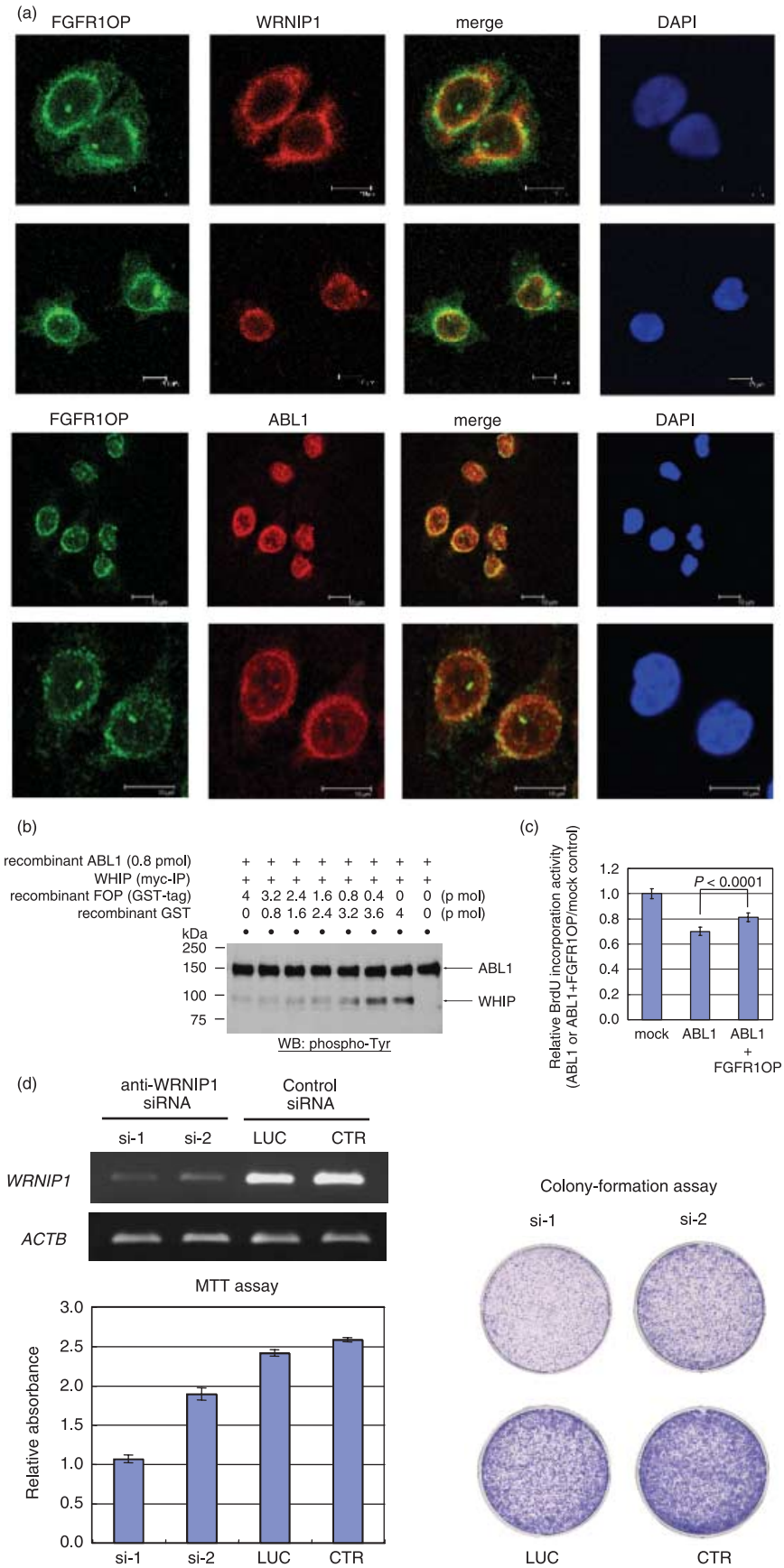

Fig. 5. Significant reduction of ABL1-dependent phosphorylation of Werner helicase interacting protein 1 (WRNIP1) by fibroblast growth factor receptor 1 oncogene partner (FGFR1OP). (a) Immunofluorescence staining of endogenous FGFR1OP and endogenous WRNIP1 in A549 cells. The FGFR1OP-Alexa488 (green), WRNIP1-Alexa594 (red), or cell nuclei (4′6′-diamidino-2-phenylindole dihydrochloride [DAPI]) were visualized. Co-localization of FGFR1OP and WRNIP1 was observed mainly in perinucleus (upper panels). Immunofluorescence staining of endogenous FGFR1OP and endogenous ABL1 in A549 cells. The FGFR1OP-Alexa488 (green), ABL1-Alexa594 (red), or cell nuclei (DAPI) were visualized. Co-localization of FGFR1OP and ABL1 was observed mainly in perinucleus (lower panels). (b) Inhibition of ABL1 kinase activity on WRNIP1 by FGFR1OP. Kinase assays were conducted by incubating c-myc-tagged WRN1IP (as substrate) with recombinant ABL1 (as kinase) in the presence of recombinant GST-tagged FGFR1OP or recombinant GST. After the kinase reaction, samples were subjected to western-blot analysis with antipan-phosphotyrosine antibodies. (c) The effect of FGFR1OP on ABL1-induced cell-cycle arrest was analyzed by BrdU incorporation assay. A549 cells were cotransfected with expression plasmids for Flag-tagged ABL1 and c-myc-tagged FGFR1OP. The cells were allowed to incorporate BrdU for the last 8 h, and its absorbancies were measured. (d) Growth promotive effect of WRNIP1. Inhibition of growth of a lung cancer cell line LC319 by siRNAs against WRNIP1. *Left upper panels,* gene knockdown effect on *WRNIP1* expression in LC319 cells by two si-WRNIP1 (si-WRNIP1-1 and si-WRNIP-2) and two control siRNAs (si-LUC [luciferase] and si-control [CTR]), analyzed by reverse transcription-polymerase chain reaction (RT-PCR). Left lower and right panels, colony formation and MTT assays of LC319 cells transfected with si-WRNIPs or control siRNAs. Columns, relative absorbance of triplicate assays; bars, SD.

chromosomal translocation, fusing FGFR1OP and FGFR1 genes, was found in cases of myeloproliferative disorder.[28–30] The resulting chimeric protein contains the N-terminal leucine-rich region of FGFR1OP protein fused to the catalytic domain of FGFR1. The LisH domain in FGFR1OP-FGFR1 fusion kinase targets the centrosome, activates signaling pathways at this organelle, and sustains continuous entry in the cell cycle.[44] However, since our study by RT-PCR using lung cancer samples detected no expression of chimeric *FGFR1OP-FGFR1*, FGFR1OP-FGFR1 fusion kinase was unlikely to contribute to lung carcinogenesis.

Our treatment of NSCLC cells with specific siRNA to reduce expression of *FGFR1OP* resulted in growth suppression, whereas induction of FGFR1OP promoted the cell growth and increased the cellular invasion activity (Fig. 3). Moreover, clinicopathological evidence through our tissue-microarray experiments demonstrated that NSCLC patients with tumors strongly expressing FGFR1OP showed shorter cancer-specific survival periods than those with negative or weak FGFR1OP expression. The results obtained by *in vitro* and *in vivo* assays strongly suggest that overexpressed FGFR1OP is likely to be an important molecule that may induce a highly malignant phenotype of lung-cancer cells. This is, to our best knowledge, the first study to show the prognostic value of FGFR1OP expression as a cancer biomarker. We should mention also that we found by our genome-wide gene expression profile database the overexpression of FGFR1OP in more than half of bladder cancer, cervical cancer, prostate cancer, renal cell cancer, and osteosarcoma (data not shown). This suggests that overexpression of FGFR1OP might play a significant role in the progression of various types of cancer as well.

We found that FGFR1OP was localized not only in the centrosome, but also in the nucleus, cytoplasm and perinucleus of lung cancer cells (Fig. 1c). These findings suggested that subcellular localization of FGFR1OP might be tightly regulated in a cell-cycle-dependent manner. Interestingly, immunocytochemical analyses revealed colocalization of FGFR1OP with its interacting proteins, WRNIP1 and ABL1, mainly in perinucleus as well as in the nucleus of NSCLC cells at S-G2/M phases (Fig. 5a). The results may suggest the significant role(s) of FGFR1OP through interaction with WRNIP1/ABL1 at this phase during cancer cell cycle progression. WRNIP1 is known to interact with the N-terminal portion of WRN. *Sgs1* and *Mgs1*, the homolog of *WRN* and *WRNIP1*, respectively, were identified in budding yeast.[33,45] Deletion of both *Sgs1* and *Mgs1* increases the rates of terminal G2/M arrest, and then leads to slow growth and shortens life span in yeast cells.[31,34] In fact, our treatment of NSCLC cells with specific siRNA to reduce expression of *WRNIP1* resulted in growth suppression, independently indicating the possible role of WRNIP in cancer cell cycle progression.

On the other hand, the ubiquitously expressed ABL1 is non-receptor tyrosine kinase distributed in the nucleus and cytoplasm.[46] Previous studies have shown that overexpression of ABL1 in Saos-2 cells, which do not express p53 or RB, can activate apoptosis and transient expression of ABL1 weakly induced apoptosis in about 10% of transfected NIH3T3 cells.[47,48] This evidence suggests that ABL1 plays an active role in the cell cycle regulation and death. In this report, we provided evidence that ABL1 could phosphorylate WRNIP1 at tyrosine residues. Interestingly, this enzymatic reaction was likely to be suppressed by FGFR1OP. Although the detailed mechanism of functional interaction among these three proteins remains to be elucidated, targeting this complex might be one of the new approaches to suppress the cancer specific cell signaling that is important for cell proliferation and/or survival.

In summary, we indicated that overexpressed FGFR1OP significantly reduced ABL1-dependent phosphorylation of WRNIP1 and resulted in the cell cycle progression of lung tumors, and that FGFR1OP could be an essential contributor to aggressive features of lung cancers.

Acknowledgment

We thank Wee-Sung Park for her excellent technical contribution to this project.

References

1 Greenlee RT, Hill-Harmon MB, Murray T, Thun M. *Cancer statistics*. *CA Cancer J Clin* 2001; **51**: 15–36.
2 Sozzi G. Molecular biology of lung cancer. *Eur J Cancer* 2001; **37** (Suppl 7): S63–73.
3 Kelly K, Crowley J, Bunn PA *et al*. Randomized phase III trial of paclitaxel plus carboplatin versus vinorelbine plus cisplatin in the treatment of patients with advanced non-small-cell lung cancer: a Southwest Oncology Group trial. *J Clin Oncol* 2001; **19**: 3210–18.
4 Schiller JH, Harrington D, Belani CP *et al*. Comparison of four chemotherapy regimens for advanced non-small-cell lung cancer. *N Engl J Med* 2002; **346**: 92–8.
5 Kikuchi T, Daigo Y, Katagiri T *et al*. Expression profiles of non-small cell lung cancers on cDNA microarrays: identification of genes for prediction of lymph-node metastasis and sensitivity to anti-cancer drugs. *Oncogene* 2003; **22**: 2192–205.
6 Kikuchi T, Daigo Y, Ishikawa N *et al*. Expression profiles of metastatic brain tumor from lung adenocarcinomas on cDNA microarray. *Int J Oncol* 2006; **28**: 799–805.
7 Kakiuchi S, Daigo Y, Tsunoda T, Yano S, Sone S, Nakamura Y. Genome-wide analysis of organ-preferential metastasis of human small cell lung cancer in mice. *Mol Cancer Res* 2003; **1**: 485–99.
8 Kakiuchi S, Daigo Y, Ishikawa N *et al*. Prediction of sensitivity of advanced non-small cell lung cancers to gefitinib (Iressa, ZD1839). *Hum Mol Genet* 2004; **13**: 3029–43.
9 Ochi K, Daigo Y, Katagiri T *et al*. Prediction of response to neoadjuvant chemotherapy for osteosarcoma by gene-expression profiles. *Int J Oncol* 2004; **24**: 647–55.
10 Yamabuki T, Daigo Y, Kato T *et al*. Genome-wide gene expression profile analysis of esophageal squamous cell carcinomas. *Int J Oncol* 2006 June; **28**: 1375–84.
11 Taniwaki M, Daigo Y, Ishikawa N *et al*. Gene expression profiles of small-cell lung cancers: molecular signatures of lung cancer. *Int J Oncol* 2006; **29**: 567–75.
12 Saito-Hisaminato A, Katagiri T, Kakiuchi S, Nakamura T, Tsunoda T, Nakamura Y. Genome-wide profiling of gene expression in 29 normal human tissues with a cDNA microarray. *DNA Res* 2002; **9**: 35–45.
13 Ochi K, Daigo Y, Katagiri T *et al*. Expression profiles of two types of human knee-joint cartilage. *J Hum Genet* 2003; **48**: 177–82.
14 Suzuki C, Daigo Y, Kikuchi T, Katagiri T, Nakamura Y. Identification of COX17 as a therapeutic target for non-small cell lung cancer. *Cancer Res* 2003; **63**: 7038–41.
15 Suzuki C, Daigo Y, Ishikawa N *et al*. ANLN plays a critical role in human lung carcinogenesis through the activation of RHOA and by involvement in the phosphoinositide 3-kinase/AKT pathway. *Cancer Res* 2005; **65**: 11 314–25.
16 Suzuki C, Takahashi K, Hayama S *et al*. Identification of Myc-associated protein with JmjC domain as a novel therapeutic target oncogene for lung cancer. *Mol Cancer Ther* 2007; **6**: 542–51.
17 Ishikawa N, Daigo Y, Yasui W *et al*. ADAM8 as a novel serological and histochemical marker for lung cancer. *Clin Cancer Res* 2004; **10**: 8363–70.
18 Ishikawa N, Daigo Y, Taniwaki M *et al*. Increases of amphiregulin and transforming growth factor-alpha in serum as predictors of poor response to gefitinib among patients with advanced non-small cell lung cancers. *Cancer Res* 2005; **65**: 9176–84.
19 Ishikawa N, Daigo Y, Takano A *et al*. Characterization of SEZ6L2 cell-surface protein as a novel prognostic marker for lung cancer. *Cancer Sci* 2006; **97**: 737–45.
20 Kato T, Daigo Y, Hayama S *et al*. A novel human tRNA-dihydrouridine synthase involved in pulmonary carcinogenesis. *Cancer Res* 2005; **65**: 5638–46.
21 Kato T, Hayama S, Yamabuki Y *et al*. Increased expression of insulin-like growth factor-II messenger RNA-binding protein 1 is associated with tumor progression in patients with lung cancer. *Clin Cancer Res* 2007; **13**: 434–42.
22 Kato T, Sato N, Hayama S *et al*. Activation of HJURP (Holliday Junction-

doi: 10.1111/j.1349-7006.2007.00610.x

Recognizing Protein) involved in the chromosomal stability and immortality of cancer cells. *Cancer Res* 2007 Sep 6; [Epub ahead of print].
23 Furukawa C, Daigo Y, Ishikawa N *et al*. Plakophilin 3 oncogene as prognostic marker and therapeutic target for lung cancer. *Cancer Res* 2005; **65**: 7102–10.
24 Takahashi K, Furukawa C, Takano A *et al*. The neuromedin u-growth hormone secretagogue receptor 1b/neurotensin receptor 1 oncogenic signaling pathway as a therapeutic target for lung cancer. *Cancer Res* 2006; **66**: 9408–19.
25 Hayama S, Daigo Y, Kato T *et al*. Activation of CDCA1-KNTC2, members of centromere protein complex, involved in pulmonary carcinogenesis. *Cancer Res* 2006; **66**: 10 339–48.
26 Hayama S, Daigo Y, Yamabuki T *et al*. Phosphorylation and activation of cell division cycle associated 8 by aurora kinase B plays a significant role in human lung carcinogenesis. *Cancer Res* 2007; **67**: 4113–22.
27 Yamabuki T, Takano A, Hayama S *et al*. Dickkopf-1 as a Novel Serologic and Prognostic Biomarker for Lung and Esophageal Carcinomas. *Cancer Res* 2007; **67**: 2517–25.
28 Popovici C, Zhang B, Gregoire MJ *et al*. The t (6;8) (q27;p11) translocation in a stem cell myeloproliferative disorder fuses a novel gene, FOP, to fibroblast growth factor receptor 1. *Blood* 1999; **93**: 1381–9.
29 Guasch G, Ollendorff V, Borg JP, Birnbaum D, Pebusque MJ. 8p12 stem cell myeloproliferative disorder: the FOP-fibroblast growth factor receptor 1 fusion protein of the t (6;8) translocation induces cell survival mediated by mitogen–activated protein kinase and phosphatidylinositol 3–kinase/Akt/mTOR pathways. *Mol Cell Biol* 2001; **21**: 8129–42.
30 Guasch G, Delaval B, Arnoulet C *et al*. FOP-FGFR1 tyrosine kinase, the product of a t (6;8) translocation, induces a fatal myeloproliferative disease in mice. *Blood* 2004; **103**: 309–12.
31 Kawabe Y, Branzei D, Hayashi T *et al*. A novel protein interacts with the Werner's syndrome gene product physically and functionally. *J Biol Chem* 2001; **276**: 20 364–9.
32 Kawabe Y, Seki M, Seki T *et al*. Covalent modification of the Werner's syndrome gene product with the ubiquitin-related protein, SUMO-1. *J Biol Chem* 2000; **275**: 20 963–6.
33 Hishida T, Iwasaki H, Ohno T, Morishita T, Shinagawa H. A yeast gene, MGS1, encoding a DNA-dependent AAA(+) ATPase is required to maintain genome stability. *Proc Natl Acad Sci USA* 2001; **98**: 8283–9.
34 Branzei D, Seki M, Onoda F, Enomoto T. The product of Saccharomyces cerevisiae WHIP/MGS1, a gene related to replication factor C genes, interacts functionally with DNA polymerase delta. *Mol Genet Genomics* 2002; **268**: 371–86.
35 Tsurimoto T, Shinozaki A, Yano M, Seki M, Enomoto T. Human Werner helicase interacting protein 1 (WRNIP1) functions as a novel modulator for DNA polymerase delta. *Genes Cells* 2005; **10**: 13–22.
36 Travis WD, Colby TV, Corrin B, Shimosato Y, Brambilla E. *Histological Typing of Lung and Pleural Tumors: World Health Organization International Histological Classification of Tumors*, 3rd edn. Berlin: Springer, 1999.
37 Chin SF, Daigo Y, Huang HE *et al*. A simple and reliable pretreatment protocol facilitates fluorescent *in situ* hybridisation on tissue microarrays of paraffin wax embedded tumour samples. *Mol Pathol* 2003; **56**: 275–9.
38 Callagy G, Cattaneo E, Daigo Y *et al*. Molecular classification of breast carcinomas using tissue microarrays. *Diagn Mol Pathol* 2003; **12**: 27–34.
39 Callagy G, Pharoah P, Chin SF *et al*. Identification and validation of prognostic markers in breast cancer with the complementary use of array-CGH and tissue microarrays. *J Pathol* 2005; **205**: 388–96.
40 Wang JY. Regulation of cell death by the Abl tyrosine kinase. *Oncogene* 2000; **19**: 5643–50.
41 Pendergast AM. The Abl family kinases: mechanisms of regulation and signaling. *Adv Cancer Res* 2002; **85**: 51–100.
42 Emes RD, Ponting CP. A new sequence motif linking lissencephaly, Treacher Collins and oral-facial-digital type 1 syndromes, microtubule dynamics and cell migration. *Hum Mol Genet* 2001; **10**: 2813–20.
43 Umeda M, Nishitani H, Nishimoto T. A novel nuclear protein, Twa1, and Muskelin comprise a complex with RanBPM. *Gene* 2003; **303**: 47–54.
44 Delaval B, Letard S, Lelievre H *et al*. Oncogenic tyrosine kinase of malignant hemopathy targets the centrosome. *Cancer Res* 2005; **65**: 7231–40.
45 Gangloff S, McDonald JP, Bendixen C, Arthur L, Rothstein R. The yeast type I topoisomerase Top3 interacts with Sgs1, a DNA helicase homolog: a potential eukaryotic reverse gyrase. *Mol Cell Biol* 1994; **14**: 8391–8.
46 Wen ST, Jackson PK, Van Etten RA. The cytostatic function of c-Abl is controlled by multiple nuclear localization signals and requires the p53 and Rb tumor suppressor gene products. *EMBO J* 1996; **15**: 1583–95.
47 Theis S, Roemer K. c-Abl tyrosine kinase can mediate tumor cell apoptosis independently of the Rb and p53 tumor suppressors. *Oncogene* 1998; **17**: 557–64.
48 Cong F, Goff SP. c-Abl-induced apoptosis, but not cell cycle arrest, requires mitogen-activated protein kinase kinase 6 activation. *Proc Natl Acad Sci USA* 1999; **96**: 13 819–24.